

NUCLEAR DATA AND MEASUREMENTS SERIES

ANL/NDM-57

**The Total, Elastic-, and Inelastic-Scattering Fast-Neutron Cross
Sections of Natural Chromium**

by

Peter T. Guenther, Alan B. Smith, and James F. Whalen

January 1981

**ARGONNE NATIONAL LABORATORY,
ARGONNE, ILLINOIS 60439, U.S.A.**

NUCLEAR DATA AND MEASUREMENTS SERIES

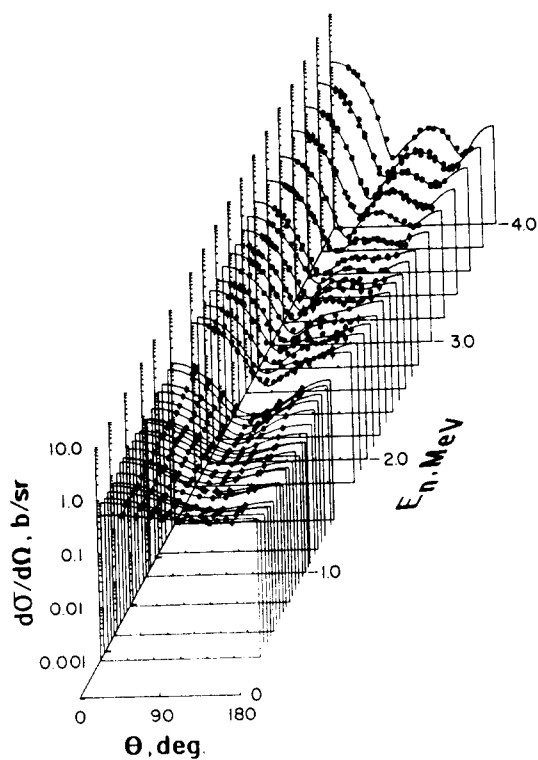
ANL/NDM-57

THE TOTAL, ELASTIC- AND INELASTIC-SCATTERING
FAST-NEUTRON CROSS SECTIONS OF NATURAL CHROMIUM

by

Peter T. Guenther, Alan B. Smith and James F. Whalen

January 1981



U of C-AUA-USDOE

ARGONNE NATIONAL LABORATORY,
ARGONNE, ILLINOIS 60439, U.S.A.

The facilities of Argonne National Laboratory are owned by the United States Government. Under the terms of a contract (W-31-109-Eng-38) between the U. S. Department of Energy, Argonne Universities Association and The University of Chicago, the University employs the staff and operates the Laboratory in accordance with policies and programs formulated, approved and reviewed by the Association.

MEMBERS OF ARGONNE UNIVERSITIES ASSOCIATION

The University of Arizona	Kansas State University	The Ohio State University
Carnegie-Mellon University	The University of Kansas	Ohio University
Case Western Reserve University	Loyola University	The Pennsylvania State University
The University of Chicago	Marquette University	Purdue University
University of Cincinnati	Michigan State University	Saint Louis University
Illinois Institute of Technology	The University of Michigan	Southern Illinois University
University of Illinois	University of Minnesota	The University of Texas at Austin
Indiana University	University of Missouri	Washington University
Iowa State University	Northwestern University	Wayne State University
The University of Iowa	University of Notre Dame	The University of Wisconsin

NOTICE

This report was prepared as an account of work sponsored by the United States Government. Neither the United States nor the United States Department of Energy, nor any of their employees, nor any of their contractors, subcontractors, or their employees, makes any warranty, express or implied, or assumes any legal liability or responsibility for the accuracy, completeness or usefulness of any information, apparatus, product or process disclosed, or represents that its use would not infringe privately-owned rights. Mention of commercial products, their manufacturers, or their suppliers in this publication does not imply or connote approval or disapproval of the product by Argonne National Laboratory or the U. S. Department of Energy.

ANL/NDM-57

THE TOTAL, ELASTIC- AND INELASTIC-SCATTERING
FAST-NEUTRON CROSS SECTIONS OF NATURAL CHROMIUM

by

Peter T. Guenther, Alan B. Smith and James F. Whalen
January 1981

Applied Physics Division
Argonne National Laboratory
9700 South Cass Avenue
Argonne, Illinois 60439
USA

NUCLEAR DATA AND MEASUREMENTS SERIES

The Nuclear Data and Measurements Series presents results of studies in the field of microscopic nuclear data. The primary objective is the dissemination of information in the comprehensive form required for nuclear technology applications. This Series is devoted to: a) measured microscopic nuclear parameters, b) experimental techniques and facilities employed in measurements, c) the analysis, correlation and interpretation of nuclear data, and d) the evaluation of nuclear data. Contributions to this Series are reviewed to assure technical competence and, unless otherwise stated, the contents can be formally referenced. This Series does not supplant formal journal publication but it does provide the more extensive information required for technological applications (e.g., tabulated numerical data) in a timely manner.

OTHER ISSUES IN THE ANL/NDM SERIES ARE:

- ANL/NDM-1 Cobalt Fast Neutron Cross Sections—Measurement and Evaluation by P. T. Guenther, P. A. Moldauer, A. B. Smith, D. L. Smith and J. F. Whalen, July 1973.
- ANL/NDM-2 Prompt Air-Scattering Corrections for a Fast-Neutron Fission Detector: $E_n \leq 5$ MeV by Donald L. Smith, September 1973.
- ANL/NDM-3 Neutron Scattering from Titanium; Compound and Direct Effects by E. Barnard, J. deVilliers, P. Moldauer, D. Reitmann, A. Smith and J. Whalen, October 1973.
- ANL/NDM-4 ^{90}Zr and ^{92}Zr ; Neutron Total and Scattering Cross Sections by P. Guenther, A. Smith and J. Whalen, July 1974.
- ANL/NDM-5 Delayed Neutron Data - Review and Evaluation by Samson A. Cox, April 1974.
- ANL/NDM-6 Evaluated Neutronic Cross Section File for Niobium by R. Howerton, Lawrence Livermore Laboratory and A. Smith, P. Guenther and J. Whalen, Argonne National Laboratory, May 1974.
- ANL/NDM-7 Neutron Total and Scattering Cross Sections of Some Even Isotopes of Molybdenum and the Optical Model by A. B. Smith, P. T. Guenther and J. F. Whalen, June 1974.
- ANL/NDM-8 Fast Neutron Capture and Activation Cross Sections of Niobium Isotopes by W. P. Poenitz, May 1974.
- ANL/NDM-9 Method of Neutron Activation Cross Section Measurement for $E_n = 5.5\text{--}10$ MeV Using the $\text{D}(d,n)\text{He-3}$ Reaction as a Neutron Source by D. L. Smith and J. W. Meadows, August 1974.
- ANL/NDM-10 Cross Sections for (n,p) Reactions on ^{27}Al , $^{46,47,48}\text{Ti}$, $^{54,56}\text{Fe}$, ^{58}Ni , ^{59}Co and ^{64}Zn from Near Threshold to 10 MeV by Donald L. Smith and James W. Meadows, January 1975.
- ANL/NDM-11 Measured and Evaluated Fast Neutron Cross Sections of Elemental Nickel by P. Guenther, A. Smith, D. Smith and J. Whalen, Argonne National Laboratory and R. Howerton, Lawrence Livermore Laboratory, July 1975.
- ANL/NDM-12 A Spectrometer for the Investigation of Gamma Radiation Produced by Neutron-Induced Reactions by Donald L. Smith, April 1975.
- ANL/NDM-13 Response of Several Threshold Reactions in Reference Fission Neutron Fields by Donald L. Smith and James W. Meadows, June 1975.
- ANL/NDM-14 Cross Sections for the $^{66}\text{Zn}(n,p)^{66}\text{Cu}$, $^{113}\text{In}(n,n')^{113\text{m}}\text{In}$ and $^{115}\text{In}(n,n')^{115\text{m}}\text{In}$ Reactions from Near Threshold to 10 MeV by Donald L. Smith and James W. Meadows, July 1975.

- ANL/NDM-15 Radiative Capture of Fast Neutrons in ^{165}Ho and ^{181}Ta by W. P. Poenitz, June 1975.
- ANL/NDM-16 Fast Neutron Excitation of the Ground-State Rotational Band of ^{238}U by P. Guenther, D. Havel and A. Smith, September 1975.
- ANL/NDM-17 Sample-Size Effects in Fast-Neutron Gamma-Ray Production Measurements: Solid-Cylinder Samples by Donald L. Smith, September 1975.
- ANL/NDM-18 The Delayed Neutron Yield of ^{238}U and ^{241}Pu by J. W. Meadows January 1976.
- ANL/NDM-19 A Remark on the Prompt-Fission-Neutron Spectrum of ^{252}Cf by P. Guenther, D. Havel, R. Sjoblom and A. Smith, March 1976.
- ANL/NDM-20 Fast-Neutron-Gamma-Ray Production from Elemental Iron: $E_n \lesssim 2$ MeV by Donald L. Smith, May 1976.
- ANL/NDM-21 Note on the Experimental Determination of the Relative Fast-Neutron Sensitivity of a Hydrogenous Scintillator by A. Smith, P. Guenther and R. Sjoblom, June 1976.
- ANL/NDM-22 Note on Neutron Scattering and the Optical Model Near $A=208$ by P. Guenther, D. Havel and A. Smith, September 1976.
- ANL/NDM-23 Remarks Concerning the Accurate Measurement of Differential Cross Sections for Threshold Reactions Used in Fast-Neutron Dosimetry for Fission Reactors by Donald L. Smith, December 1976.
- ANL/NDM-24 Fast Neutron Cross Sections of Vanadium and an Evaluated Neutronic File by P. Guenther, D. Havel, R. Howerton, F. Mann, D. Smith, A. Smith and J. Whalen, May 1977.
- ANL/NDM-25 Determination of the Energy Scale for Neutron Cross Section Measurements Employing a Monoenergetic Accelerator by J. W. Meadows, January 1977.
- ANL/NDM-26 Evaluation of the $\text{IN-115}(\text{N},\text{N}')\text{IN-115M}$ Reaction for the ENDF/B-V Dosimetry File by Donald L. Smith, December 1976.
- ANL/NDM-27 Evaluated (n,p) Cross Sections of ^{46}Ti , ^{47}Ti and ^{48}Ti by C. Philis and O. Bersillon, Bruyeres-le-Chatel, France and D. Smith and A. Smith, Argonne National Laboratory, January 1977.
- ANL/NDM-28 Titanium-II: An Evaluated Nuclear Data File by C. Philis, Centre d'Etudes de Bruyères-le-Châtel, R. Howerton, Lawrence Livermore Laboratory and A. B. Smith, Argonne National Laboratory, June 1977.
- ANL/NDM-29 Note on the 250 keV Resonance in the Total Neutron Cross Section of ^6Li by A. B. Smith, P. Guenther, D. Havel and J. F. Whalen, June 1977.

- ANL/NDM-30 Analysis of the Sensitivity of Spectrum-Average Cross Sections to Individual Characteristics of Differential Excitation Functions by Donald L. Smith, March 1977.
- ANL/NDM-31 Titanium-I: Fast Neutron Cross Section Measurements by P. Guenther, D. Havel, A. Smith and J. Whalen, May 1977.
- ANL/NDM-32 Evaluated Fast Neutron Cross Section of Uranium-238 by W. Poenitz, E. Pennington, and A. B. Smith, Argonne National Laboratory and R. Howerton, Lawrence Livermore Laboratory, October 1977.
- ANL/NDM-33 Comments on the Energy-Averaged Total Neutron Cross Sections of Structural Materials by A. B. Smith and J. F. Whalen, June 1977.
- ANL/NDM-34 Graphical Representation of Neutron Differential Cross Section Data for Reactor Dosimetry Applications by Donald L. Smith, June 1977.
- ANL/NDM-35 Evaluated Nuclear Data File of Th-232 by J. Meadows, W. Poenitz, A. Smith, D. Smith and J. Whalen, Argonne National Laboratory and R. Howerton, Lawrence Livermore Laboratory, February 1978.
- ANL/NDM-36 Absolute Measurements of the $^{233}\text{U}(n,f)$ Cross Section Between 0.13 and 8.0 MeV by W. P. Poenitz, April 1978.
- ANL/NDM-37 Neutron Inelastic Scattering Studies for Lead-204 by D. L. Smith and J. W. Meadows, December 1977.
- ANL/NDM-38 The Alpha and Spontaneous Fission Half-Lives of ^{242}Pu by J. W. Meadows, December 1977.
- ANL/NDM-39 The Fission Cross Section of ^{239}Pu Relative to ^{235}U from 0.1 to 10 MeV by J. W. Meadows, March 1978.
- ANL/NDM-40 Statistical Theory of Neutron Nuclear Reactions by P. A. Moldauer, February 1978.
- ANL/NDM-41 Energy-Averaged Neutron Cross Sections of Fast-Reactor Structural Materials by A. Smith, R. McKnight and D. Smith, February 1978.
- ANL/NDM-42 Fast Neutron Radiative Capture Cross Section of ^{232}Th by W. P. Poenitz and D. L. Smith, March 1978.
- ANL/NDM-43 Neutron Scattering from ^{12}C in the Few-MeV Region by A. Smith, R. Holt and J. Whalen, September 1978.
- ANL/NDM-44 The Interaction of Fast Neutrons with ^{60}Ni by A. Smith, P. Guenther, D. Smith and J. Whalen, January 1979.
- ANL/NDM-45 Evaluation of $^{235}\text{U}(n,f)$ between 100 KeV and 20 MeV by W. P. Poenitz, July 1979.

- ANL/NDM-46 Fast-Neutron Total and Scattering Cross Sections of ^{107}Ag in the MeV Region by A. Smith, P. Guenther, G. Winkler and J. Whalen, January 1979.
- ANL/NDM-47 Scattering of MeV Neutrons from Elemental Iron by A. Smith and P. Guenther, March 1979.
- ANL/NDM-48 ^{235}U Fission Mass and Counting Comparison and Standardization by W. P. Poenitz, J. W. Meadows and R. J. Armani, May 1979.
- ANL/NDM-49 Some Comments on Resolution and the Analysis and Interpretation of Experimental Results from Differential Neutron Measurements by Donald L. Smith, November 1979.
- ANL/NDM-50 Prompt-Fission-Neutron Spectra of ^{233}U , ^{235}U , ^{239}Pu and ^{240}Pu Relative to that of ^{252}Cf by A. Smith, P. Guenther, G. Winkler and R. McKnight, September 1979.
- ANL/NDM-51 Measured and Evaluated Neutron Cross Sections of Elemental Bismuth by A. Smith, P. Guenther, D. Smith and J. Whalen, April 1980.
- ANL/NDM-52 Neutron Total and Scattering Cross Sections of ^6Li in the Few MeV Region by P. Guenther, A. Smith and J. Whalen, February 1980.
- ANL/NDM-53 Neutron Source Investigations in Support of the Cross Section at the Argonne Fast-Neutron Generator by James W. Meadows and Donald L. Smith, May 1980.
- ANL/NDM-54 The Nonelastic-Scattering Cross Sections of Elemental Nickel by A. B. Smith, P. T. Guenther and J. F. Whalen, June 1980.
- ANL/NDM-55 Thermal Neutron Calibration of a Tritium Extraction Facility using the $^6\text{Li}(n,t)^4\text{He}/^{197}\text{Au}(n,\gamma)^{198}\text{Au}$ Cross Section Ratio for Standardization by M. M. Bretscher and D. L. Smith, August 1980.
- ANL/NDM-56 Fast-Neutron Interactions with ^{182}W , ^{184}W and ^{186}W by P. T. Guenther, A. B. Smith and J. F. Whalen, December 1980.

TABLE OF CONTENTS

	<u>Page</u>
LIST OF FIGURES.....	vii
LIST OF TABLES.....	viii
ABSTRACT.....	ix
I. INTRODUCTION.....	1
II. EXPERIMENTAL METHODS.....	3
A. Measurement Samples.....	3
B. Neutron Total Cross Sections.....	3
C. Neutron Scattering Measurements.....	4
III. EXPERIMENTAL RESULTS.....	6
A. Neutron Total Cross Sections.....	6
B. Neutron Elastic Scattering.....	8
C. Neutron Inelastic Scattering.....	10
IV. INTERPRETATION.....	14
V. CONCLUSIONS.....	19
ACKNOWLEDGMENT.....	20
REFERENCES.....	21
FIGURE CAPTIONS.....	24
FIGURES 1-6.....	25-30

LIST OF FIGURES

<u>No.</u>	<u>Title</u>	<u>Page</u>
Fig. 1.	Extrapolation of Effective Neutron Total Cross Sections.	
a)	The lower portion of the figure shows the extrapolated energy-averaged cross sections of elemental Cr as stars, those of the Cr ENDF/B-V as squares (see text for details). The upper portion of the figure details the linear fit to the effective cross sections at each energy point as deviation from the extrapolated (i.e., "zero thickness") values in percent vs. sample thickness (nuclei per barn)....	25
b)	Simulated extrapolation derived from the Cr ENDF/B-V total cross sections using the energy resolution of the present work.....	25
c)	As in b) but using the high-resolution Fe data of [28].....	25
d)	As in c) but with a 10 keV resolution.....	25
Fig. 2.	Neutron Total- and Elastic-Scattering Cross Sections of Elemental Chromium. The present results are indicated by 0 and \square , those of [3] by x, those of [4] by +. The light curves are the corresponding appropriately averaged ENDF/B-V values. The heavy curves are the results of model calculations of this work.....	26
Fig. 3.	Neutron Elastic-Scattering Angular Distributions for Elemental Chromium. The curves are Legendre polynomial least-squares fits to the combined experimental data. (Units: Barns per steradian in laboratory degrees.).....	27
Fig. 4.	Neutron Elastic-Scattering Angular Distributions for Elemental Chromium. The results of this work (0) are compared with those of [3] (x) and [4] (+) at selected incident-neutron energies. The parenthetical energy values pertain to [4]. The curves are least-squares Legendre polynomial fits to the ± 200 keV average of the present data. (Units: Barns per steradian in laboratory degrees.).....	28
Fig. 5.	Neutron Inelastic-Scattering from Elemental Chromium. The cross sections of this work (0) are compared with those of [3] (x), those of [7] (+), and summed entries from ENDF/B-V as described in the text (light curves). The heavy curves are the results of model calculations of this work.....	29
Fig. 6.	Neutron Elastic-Scattering Angular Distributions for Elemental Chromium. Experimental data of this work have been averaged over ± 200 keV intervals and are indicated by 0. The curves are the results of model calculations of this work. (Units: Barns per steradian in laboratory degrees.).....	30

LIST OF TABLES

<u>No.</u>	<u>Title</u>	<u>Page</u>
I.	Observed Inelastic - Neutron Excitations in Elemental Chromium.....	11
II.	Optical-Model Parameters.....	17

THE TOTAL, ELASTIC- AND INELASTIC-SCATTERING
FAST-NEUTRON CROSS SECTIONS OF NATURAL CHROMIUM*

by

Peter T. Guenther, Alan B. Smith and James F. Whalen

Applied Physics Division
Argonne National Laboratory
9700 South Cass Avenue
Argonne, Illinois 60439

ABSTRACT

Neutron total cross sections of natural chromium were measured from 1.0 to 4.5 MeV with intermediate energy resolution at intervals of $\lesssim 50$ keV. Elastic- and inelastic-differential-scattering cross sections were determined over the energy and angular range of 1.5 - 4.0 MeV and 20 - 160 degrees, respectively. Cross sections were measured for inelastic-excitation neutron-groups corresponding to average Q-values of: 1.433 ± 0.009 , 2.377 ± 0.008 , 2.665 ± 0.005 , 2.778 ± 0.007 and 2.970 ± 0.006 MeV. The results were examined in terms of the spherical optical-statistical model. The contribution of vibrational direct-excitation to the 1.433 state was assessed.

*This work was supported by the U.S. Department of Energy.

I. INTRODUCTION

Chromium is an important constituent of radiation and heat resistant alloys, such as stainless steel, which find wide application in the neutronic design of fission and fusion systems. The natural element consists of 4.3% ^{50}Cr , 83.8% ^{52}Cr , 9.5% ^{53}Cr , and 2.4% ^{54}Cr , and thus the fast-neutron interactions with ^{52}Cr predominate in general.

Fast-neutron total and scattering cross sections of chromium have been previously investigated (e.g. Refs. 1-13). A strong motivation for undertaking this work was the desire to obtain a comprehensive set of total and scattering cross sections of comparable, intermediate energy resolutions. This is particularly important as the ^{52}Cr cross sections display pronounced energy fluctuations in the present energy range (1-4 MeV). While intermediate energy resolutions still evince residual structure, they are nonetheless most generally useful for neutronic calculations as well as comparisons with energy-averaged nuclear models in the MeV region.

Energy dependent fluctuations complicate the analysis and interpretation of experimental measurements. They affect the various cross sections of this work in different ways. A few principal concerns are enumerated:

Any finite-sample measurement that does not completely resolve the resonance structure in fact only determines an effective total cross section. The magnitude of this cross section decreases with increasing sample thickness and the degree to which this occurs is a function of the underlying resonance structure and the experimental resolution. The importance of extrapolating the effective cross section to the true energy-averaged cross section has been recently re-emphasized [14]. As this effect is particularly severe in the present mass-energy range, the measurements of this work pay careful attention to this correction.

Fluctuations also reflect upon the definition of angular distributions. Even for elastic scattering in the present context the energy-average compound contribution amounts to some 20 - 50% of the observed cross section. One would expect, therefore, strong fluctuations in scattered-neutron angular-distribution shapes as well as magnitudes. Experimental observations bear this out. As a consequence the interpretation of a few, isolated distributions can be misleading in the definition of the elastic-scattering cross sections, and the use of closely spaced observations is implied.

The energy-dependent fluctuations of the compound nuclear cross section have, of course, an even greater impact on the inelastic excitations and this has been pointed out by previous investigators [13]. However, often, evaluated inelastic excitation functions are given a smooth behavior with energy (see for example [15]). Since many of these are small and uncertain such treatment is not necessarily inappropriate except when their sum is then used to infer (by subtraction from the total cross section) the elastic cross section. This manipulation endows the elastic scattering with energy-dependent structure that is not only inaccurate in detail but also is in excess of that attributable to the compound-elastic component. Such a shortcoming is unacceptable particularly in view of the fact that contemporary elastic scattering measurements are capable of better accuracies than those typical of inelastic results.

The above examples illustrate the need for a coherent treatment of the energy resolution when assembling a comprehensive data base descriptive of a nucleus in a mass-energy region subject to energy-dependent fluctuations. The principle goal of this work is to provide such a consistent set of total, elastic and inelastic fast-neutron-scattering cross sections suitable for defining energy-averages so important for engineering applications as well as comparison with optical-statistical models.

II. EXPERIMENTAL METHODS

A. Measurement Samples

The neutron-scattering and -total cross section measurements employed samples pressed into right cylinders from chemically pure (99.99%) elemental chromium powder [16]. A single sample (2 cm diameter by 2 cm length) was used for the scattering experiments. However, the total cross section determination required several sample thicknesses to correct for the resonance self-shielding effect. In all, eight samples were employed. These ranged from 0.033 to 0.37 atoms/barn with an uncertainty of $<1/3\%$. Sample density uniformity was verified by comparing the density of several samples before and after cutting them into pieces.

B. Neutron Total Cross Sections

The neutron total cross section measurements were performed with the monoenergetic-source facilities at the Argonne National Laboratory Fast Neutron Generator [17]. The ${}^7\text{Li}(p,n){}^7\text{Be}$ reaction with incident proton pulses of ~ 1 nsec duration at a 2 MHz repetition rate provided neutron bursts whose energy resolution was controlled by the lithium-target film thickness. A massive shield surrounded the source and collimated zero-degree-reaction neutrons to a beam ~ 1 cm in diameter at the sample position. Chromium samples of varying thickness, a carbon reference and a void were mounted (sample axis parallel to the beam) on a wheel which cycled the samples into the beam line at ~ 20 rpm. This obviated the need for flux monitoring. Further, concurrent transmission measurement of the various sample thicknesses (as well as the carbon reference) provided parameter adjustment in the resonance self-shielding correction.

Neutron selection was done by time-of-flight using a proton-recoil scintillator placed at flight paths of 5 to 8 m. The resultant time spectra were sorted by sample and stored with an on-line computer facility. The sample transmissions was obtained from the summation of the primary neutron-source peak which was well resolved from the secondary neutron-source peak. The small background was determined by linear interpolation and deadtime corrections were derived from a random-tagged signal introduced into the data acquisition system. The resultant transmissions were reduced to cross sections in the conventional manner [19].

The energy scale was calibrated to ~ 10 keV by observing the resonance structure of sulfur, silicon, and carbon [20, 21 and 22] employing the identical apparatus but with a target thickness of 2-5 keV. A detailed account of the experimental method outlined above is to be found in [18].

C. Neutron Scattering Measurements

The neutron scattering measurements were made using the Argonne National Laboratory 10-angle, pulsed beam time-of-flight system [23]. The ${}^7\text{Li} (p,n){}^7\text{Be}$ neutron source was pulsed at 2 MHz with a burst duration of ~ 1 nsec. The sample was placed (sample axis perpendicular to the scattering plane) ~ 13 cm from the neutron source at the zero-degree reaction-angle. Proton-recoil scintillators viewed the sample at flight paths of ~ 5 m through massive collimators distributed over an angular range of 20 - 160° . Relative source fluence was determined by a time-of-flight monitor as well as back-up "long counters". The relative energy dependence of the detectors was established with respect to the neutron spectrum emitted during the spontaneous fission of ${}^{252}\text{Cf}$ [24]. This sensitivity was normalized by observing neutron scattering from hydrogen, (polyethylene) at selected energies and angles. Thus all scattering cross sections were determined relative to well known $\text{H}(n;n)$ cross sections [25].

Data acquisition was accomplished with an on-line computer system. The reduction of the measured velocity spectra to differential cross sections included analytical as well as Monte-Carlo corrections for experimental effects such as angular resolution, sample attenuation and multiple-scattering. The concurrent determination of elastic angular distributions for carbon, treated by identical methods, served as a test for overall system performance. The methods outlined above are detailed in Refs. [23] and [26].

III. EXPERIMENTAL RESULTS

A. Neutron Total Cross Sections

The results reported here derive from several sets of data covering the energy range from ~ 1 to 4.5 MeV and resolutions from 50 to 100 keV. Thus the resolution of the pronounced resonance structure in chromium was purposely avoided. The progression through the energy range was arranged in overlapping increments. For a given sample, the measurements from all sequences reproduced cross section magnitudes and residual resonance structure within counting statistics which ranged from $\sim 3\%$ for the thinnest sample in worst cases to $< 1\%$ for the thickest samples. Further, all accompanying carbon cross sections were consistently in good agreement with those reported in the literature [20].

As stated in Section I, the present measurements resulted in "effective" total cross sections. Although the thin-sample cross sections were subject to greater statistical fluctuations, the reduction of cross section with sample thickness was clearly in evidence amounting to 10% or more near 1 MeV incident neutron energy and becoming negligible above approximately 3.5 MeV. In the first approximation, this reduction is linear in sample thickness. (The proportionality factor being essentially the variance of the cross section fluctuations with incident neutron energy.) The data revealed these additional properties of the sample-thickness correction below 2 MeV: First, the reduction showed a small but discernible variation with the target thickness (i.e. the energy resolution) from one data set to the next. Secondly, aside from the gross energy-dependent behavior noted above, the reduction evinced strong local fluctuations. Finally, when taken over a sufficiently wide range, the reduction was not always linear in sample thickness. Unfortunately the thin-sample data was not sufficiently precise to define the

rapidly fluctuating, small curvature. As a consequence of the foregoing observations, the measured effective cross sections were linearly extrapolated to the energy-averaged (i.e. zero-thickness) cross section for each data set and at each energy. This procedure is illustrated in Fig. 1a in detail for a Cr measurement with an energy resolution of ~ 50 keV over a small energy interval (1-1.5 MeV). A linear least-squares fit was used to approximate the true sample-thickness dependence, which is a function of the underlying resonance structure.

The experimentally observed properties of the sample-thickness correction were also explored using computer-simulated effective cross sections. In Fig. 1b, for example, they were derived from energy-averaged transmissions for various sample thicknesses at the appropriate energy resolution computed with the Cr ENDF/B-V [27] total cross section under the assumption that the latter fully resolves the energy-dependent structure. It is apparent that in this case the dependence on sample thickness is appreciably weaker and more uniform in energy than in the present experiment. This would indicate that perhaps the underlying structure is not fully resolved and that in fact the file contains an effective cross section. In contrast, as indicated in Fig. 1c, an identical simulation based on the high-resolution Fe total cross section of Harvey [28] is qualitatively similar to the present experiment. As the resolution becomes finer the overall correction becomes smaller. However, there are dramatic fluctuations in its behavior as Fig. 1d attests. Here the simulation was done in the same manner as above except with an energy resolution of 10 keV.

All data sets were extrapolated to the zero-thickness cross section as detailed in Fig. 1a. The resultant energy-averaged cross sections were then further averaged over a 200 keV interval and finally all sets were combined

in the weighted average shown in Fig. 2. The statistical errors are $<1\%$; however, due to the linear extrapolation process, the cross sections below ~ 1.5 MeV may be under-corrected by an estimated 1 to 2%. The total cross section of the Cr ENDF/B-V was averaged in the corresponding manner and is also shown in Fig. 2. Evidently, the residual fluctuations of the present work and those of the ENDF curve are very similar. Overall, the energy-averaged cross section magnitude is also in good agreement.

B. Neutron Elastic Scattering

Elastic distributions were obtained at incident neutron energies of 1.5 to 4.0 MeV in steps of 50 keV. Broad resolutions of 50 to 100 keV were secured with suitably thick target films. The energy scale was uncertain to less than 20 keV. At least ten angles were observed ranging from 20 to 160 degrees. The relative angular determinancy was $\sim 1/2^\circ$, the absolute uncertainty $\sim 1^\circ$. Individual elastic differential cross sections had an estimated overall uncertainty of 5 to 7%. Of this, counting statistics contributed 1 to 3%, geometric, multiple-scattering and other corrections a similar amount, and detector calibrations 3 to 5%. The uncertainty in the $H(n,n)$ standard is small ($\lesssim 1\%$).

The results reported here are the composite of three measurement periods. The resolution of the first set was somewhat finer (50 to 80 keV) than that of the second and third (70 to 100 keV), and therefore, the earlier distributions exhibited somewhat more pronounced fluctuations. All distributions at a given nominal energy (i.e., 20 to 40 differential values) were interpolated to a standard angle set and then averaged, with the attendant reduction of statistical uncertainty. The Legendre-polynomial least-squares fits to the resultant distributions clearly demonstrate residual shape fluctuations as

indicated in Fig. 3. To obtain a better energy average, suitable for comparison with nuclear model calculations, the running 200 keV average shown in Fig. 6 was constructed. These latter distributions were least-squares fitted with a Legendre polynomial series. The thusly derived integral values have an estimated uncertainty of 3 to 5% and are shown in Fig. 2.

There are a number of neutron-elastic-scattering distributions measured by other investigators. A single distribution by Salnikov [5] at 2.35 MeV is in fair agreement, while the one at 3.2 MeV by Becker et al. [6] is in excellent agreement with this work. The results of Holmquist and Wielding [4] and Pasechnic et al. [3] are more extensive. A comparative sampling of these and the present data is given in Fig 4. The shape agreement is generally good. The greatest disagreement occurs at 2.5 MeV where no corroboration is evident over the entire angular range. These discrepancies in detail are, at least in part, explained by differences among the various measurements in incident neutron energy and resolution. They illustrate the remarks made in Section I regarding the need for closely spaced measurements of fluctuating cross sections.

An inspection of Fig. 2 reveals that over most of the energy range depicted the present integral elastic cross sections are smaller than those of ENDF/B-V. The latter were defined as the difference between the total and non-elastic cross sections [15]. Hence, if the present data are self-consistent, the discrepancies noted here should have counterparts in the comparison of the present and ENDF/B-V inelastic-scattering cross sections. This is indeed the case as it will be seen below.

C. Neutron Inelastic Scattering

The inelastic-scattering cross sections reported in this work were obtained concurrently with the elastic distributions discussed above and, due to limited energy resolution, correspond to the excitation of close lying levels of the several isotopes of chromium as indicated in Table I. The most significant "contaminants" arise from ^{53}Cr . The contributions from minority isotopes are small and their complete inclusion during peak-summing of the inelastic groups was not always assured. Because of this and relatively poorer counting statistics, the inelastic cross sections are less certain.

In deriving the inelastic integral values, no less than four and more typically 10-20 differential cross sections were fitted with a low-order (≤ 3) least-squares Legendre polynomial. For multi-isotopic groups composed of levels with spins greater than zero, the associated angular distributions were found to be essentially isotropic. (Hauser-Feshbach calculations bear this observation out). In the case of the 2647 keV (0^+) level in ^{52}Cr , however, several distributions did confirm the characteristic concave shape which is predicted by the Hauser-Feshbach statistical model [29]. In order to provide a more consistent determination of the integral cross sections for this level, the calculated shapes were normalized to those data whose definition was insufficient to yield a satisfactory Legendre polynomial fit. The overall errors for the integrated cross sections were estimated to be 7-10% for the 1434 keV level and 15-20% for the higher excitations. The corresponding inferred angle-integrated values displayed fluctuations and were further averaged over 200 keV intervals. These results together with other reported (n,n') work, the corresponding ENDF/B-V values, and the present model calculations are shown in Fig. 5. The latter will be discussed in

Table I. Observed Inelastic - Neutron Excitations in Elemental Chromium

No.	E_x (MeV)	dE_x (MeV)	E_x (MeV) ^a	Isotopic Identifications
1	1.433	0.009	1.434	Cr-52 (2+)
2	2.377	0.008	2.321	Cr-53 (3/2-)
			2.370	Cr-52 (4+)
			2.455	Cr-53
3	2.665	0.005	2.620	Cr-54 (2+)
			2.647	Cr-52 (0+)
			2.661	Cr-53 (5/2-)
			2.670	Cr-53
			2.711	Cr-53
4	2.778	0.007	2.768	Cr-52 (4+)
			2.775	Cr-53
			2.826	Cr-53
			2.829	Cr-54 (0+)
5	2.970	0.006	2.922	Cr-50 (2)
			2.965	Cr-52 (2+)
			2.995	Cr-53

^aTaken from Ref. [30]

Section IV. Since the inelastic-scattering cross sections of ENDF/B-V are based essentially on $(n;n',\gamma)$ measurements, it will be assumed here that they are representative of such work.

The 1434 keV (2+) state was the only level fully resolved in this work and hence allows an unambiguous comparison with other work. The isotopic results of Pasechnic et al. [3] are in excellent agreement with the present results when adjusted for the isotopic abundance of ^{52}Cr , while the elemental cross sections of Almén-Ramström [7] are substantially lower below ~ 3.3 MeV. The ENDF/B-V values do not display the residual fluctuations of this work between 2 and 3 MeV. They also appear to be lower (below 2 MeV) than the expected extrapolation of the present excitation function. Above ~ 3 MeV the agreement with this work is very good.

The only other neutron measurement pertains to the 2377 keV (4+) "state". Here the single, isotopic point of Pasechnic et al. [3] is somewhat below an extrapolation of the present results. However, the inclusion of minority-isotope excitations would augment its value by 10-15%.

For comparison with the observed, multi-isotopic excitations (i.e. $E_x \gtrsim 2377$ keV) the appropriate entries of the ENDF/B-V file were summed. As Fig. 5 indicates, all these composite cross sections lie more or less below the present values. These discrepancies are not accounted for by reasonable estimates of the small contributions from ^{54}Cr to the excitations at 2665 and 2778 keV which have not been included in the file. It is interesting to correlate the differences between the present inelastic-scattering cross sections and ENDF/B-V noted here with those discussed previously in connection with the elastic cross sections. The excess elastic-scattering of ENDF/B-V is very clearly the result of underestimated inelastic-scattering. (Specifically: For $E_n \approx 2$ MeV the 1433 keV excitation is primarily at fault,

while for $E_n \gtrsim 2.5$ MeV the systematically underestimated higher excitations are responsible.) The summation of the present scattering cross sections including estimates for unmeasured excitations reproduces the independently determined total cross section within the respective experimental uncertainties.

IV. INTERPRETATION

The present experimental results were examined in terms of the optical-statistical model [29, 31]. The spherical computations were carried out with the code ABAREX [32], while the coupled-channel computations employed the code JUPREX [33]. For model comparison purposes the data were assumed to be representative of ^{52}Cr (84% abundance). This necessarily limited the rigor to be expected of the calculational results and shortcomings will be discussed. In addition, all cross sections displayed fluctuations with incident neutron energy which could be smoothed only to a degree by averaging the data over ± 200 keV intervals. Wider intervals introduce uncertainties due to edge effects and, more importantly, due to the onset of inelastic channels. Furthermore, it is not at all clear how well the data represent an energy-averaged cross section in the optical model context. For, aside from the obvious residual structure with a period of a few hundred keV, there may be superimposed undulations on the MeV scale that would be much more difficult to assess over the limited energy range of this work. These difficulties are well known in the present mass - energy range [34] and a critique of the calculational results should bear the above limitations in mind.

The spherical optical model parameterization was principally guided by the simultaneous Chi-square fitting of elastic- and inelastic-scattering angular distributions, allowing all real, imaginary and spin-orbit parameters to vary. The resultant calculated total cross section did not reproduce well the overall energy dependence exhibited by the experimental data. In particular, it was difficult to calculate a sufficiently large total cross section above ~ 3 MeV without seriously reducing the compound nuclear cross

section. A reasonable energy variation of the imaginary potential did not help, but the situation was improved slightly by introducing an additional, quadratic energy dependence in the real potential. The final parameter set is given in Table II. It should not be used outside the mass-energy range of this work. The small imaginary radius seemed to indicate the need for a volume imaginary term; however, its inclusion in the imaginary potential neither improved the fit nor increased the imaginary radius. The total cross section computed with the parameters of Table II is shown in Fig. 2. As it will become clear in connection with the partial cross sections below, the compound nuclear component is slightly overcalculated below 2 MeV and very slightly undercalculated above 3 MeV. In view of the difficulty concerning the definition of energy averages discussed above, this 3-5% discrepancy was judged acceptable.

In Fig. 6 the 200 keV-averaged data are compared with the model calculated elastic angular distributions. The residual fluctuations (in shape as well as magnitude) about the calculations are evident. For example, the second maximum, which appears rather quickly near 3 MeV in the data, evolves more gradually in the calculations. For $E_n \lesssim 2$ MeV the calculated angular distributions lie somewhat above the data. In addition to the overcalculation of the absorption cross section discussed above, the compound-elastic contribution is too large as the low-lying levels of the minority isotopes are not represented in the Hauser-Feshbach computation. These contributions amount to some 150 mb and affect both the elastic- and 1434 keV level inelastic-scattering cross sections. If these compound-nuclear cross sections are reduced in proportion to their magnitudes by the above amount, the calculations show marked improvement.

The angular distributions for the inelastic scattering to the 1434 keV state are in good agreement with the shape predicted by the Hauser-Feshbach statistical model (i.e. a slight secondary maximum near 120°) except for fluctuations in magnitude not consistent with this energy-averaged model. However, above ~ 3.6 MeV the distributions evinced a forward peaking in excess of that due to the center of mass to laboratory system transformation. This suggested the inclusion of a direct inelastic process. A Chi-square fit to the elastic- and 1434 keV inelastic-scattering angular distributions simultaneously, using JUPREX [33] assuming a one-phonon vibrational coupling scheme, produced a simple convex distribution without the secondary maximum observed experimentally. Moreover, its angle-integrated cross-section was less than that computed spherically, and the elastic-scattering angular distribution also departed from the experimental values. A rotational calculation, which had been used with success in the case of iron [35], was also considered. While this resulted in a larger direct component, the 1434 keV inelastic-scattering angular distribution still did not reproduce the characteristic secondary maximum. From these results it was concluded that the coupled-channel calculations did not improve upon the spherical optical model interpretation of the experiment. Thus the integral, elemental values of the spherical calculation are compared with the experimental cross sections in Fig. 5. As mentioned in the previous paragraph, both the overcalculated absorption as well as ignored minority levels render this calculation somewhat high for $E_n \lesssim 2$ MeV.

The calculations for the higher inelastic excitation functions are also given in Fig. 5. For a more ready comparison with the data, the calculated, elemental cross-sections were augmented by the contributions from minority isotopes as defined in Table I. These were taken from the ENDF/B-V

Table II. Optical-Model Parameters

Real Strength ^a	$52.1 - 0.3E - 0.14E^2$, MeV
Real Radius	$1.21 \cdot A^{1/3}$, F
Real Diffuseness	0.62, F
Imaginary Strength ^b	8.0, MeV
Imaginary Radius	$1.10 \cdot A^{1/3}$, F
Imaginary Diffuseness	0.60, F
Spin-orbbit Strength ^c	9.0, MeV

^aSaxon form

^bSaxon derivative form

^cThomas form

file, where available, or calculated assuming the potential in Table II and amounted to at most ~15% ($E_x = 2.665$ MeV). In all cases the calculations lie at least somewhat below the data and this is again readily explained by the deficiency in the absorption cross section discussed above. Only the calculated cross section for the 2778 keV excitation falls outside experimental error. The short fall is greater than the uncertainty arising from minority contributions. A trial calculation with smaller spin assignments yielded a result in excess of the experimental cross section. There appears to be no satisfactory explanation for the disagreement.

While the model calculations presented here are perhaps discrepant in some detail as noted, they are none-the-less remarkably successful in describing the present experimental work. This is so, in particular, despite their simple assumptions and the energy-fluctuating cross sections involved. The calculational results give credence to the self-consistency of this data base and support the remarks made in previous sections regarding the components of the chromium ENDF/B-V file.

V. CONCLUSIONS

The present results constitute the most comprehensive experimental neutron scattering data base for elemental Cr in the energy range 1.5 - 4.0 MeV available today. Together with the intermediate resolution total cross sections reported here, they provide a good basis for comparison with model calculations. None-the-less, due to the fluctuating nature of the cross sections involved, the definition of appropriate energy-averaged cross sections is difficult if not impossible because of superimposed intermediate structure. The consequences of these fluctuations and attendant complications in data analysis and interpretation will be briefly reviewed. First, all finite-sample total cross section measurements result in effective cross sections which must be corrected to yield the zero-thickness energy-averaged cross section. In this work this was done by concurrent multiple sample-thickness measurements which were then linearly extrapolated to the zero thickness cross section. It was noted in connection with this procedure that the resultant sample-thickness correction, while converging on the average with energy, showed marked local fluctuations necessitating an energy by energy treatment. Further, the cross sections, even after averaging over wider energy intervals, retained undulations which complicated comparison with model calculations. Secondly, in connection with elastic-scattering angular distributions, the difficulty of comparison with isolated measurements of other authors as well as model predictions was observed. Finally, fluctuations were also in evidence in inelastic-scattering excitation functions which made intercomparison with and/or normalization to individual measurements difficult if not simply false. In addition they complicate or perhaps invalidate such procedures as deriving partial

cross-sections as the difference between fluctuating constituents. For example, the so derived elastic scattering cross section of ENDF/B-V is in disagreement with the present results over much of the present energy range.

The summary comparison of the chromium ENDF/B-V values with the cross sections of this work is as follows: The total cross section in overall magnitude and energy dependence is in good agreement. There are small local structural differences, but these may well arise from details of energy averaging and/or scaling. The elastic-scattering cross sections, as noted above, are substantially larger than the present, independently derived results. The inelastic-scattering excitation-function for the 1433 keV level agrees well for $E_n \gtrsim 3$ MeV. Below this energy, however, neither the residual structure nor the cross section magnitude of this work are in evidence. For a comparison of the remaining inelastic excitations reported here it was necessary to sum appropriate components of the file. Without exception the group cross sections derived from ENDF/B-V fell short of present, measured values.

Finally, the model calculations reproduced the results of the experimental work reasonably well. The greatest difficulty experienced was the quantitative representation of the total cross section in concert with the appropriate absorption cross section. It is surmized that broad residual fluctuations in the compound nuclear process are responsible for these difficulties. More importantly, however, these calculations provided a check on the self-consistency of the experimental results of this work and gave support to the conclusions drawn from it.

ACKNOWLEDGMENT

This work supported by the U.S. Department of Energy.

REFERENCES

1. L. Cranberg and J. S. Levin, Phys. Rev., 103, 343 (1956).
2. Yu. G. Degtyarev and V. N. Protopopov, Sov. J. At. Energy, 23, 1350 (1967).
3. M. V. Pasechnic, M. B. Fedorov, T. I. Yakovenko, I. E. Kashuba, and V. A. Korzh, Uk. Fiz. Zh., 14, 1874 (1969).
See also
I. A. Korzh, V. A. Mishchenko, E. N. Mozhzhukhin, M. V. Pasechnic, N. M. Pravdiyoi and I. E. Sanghurt, Sov. J. Nucl. Phys., 26(6), 608 (1977).
M. V. Pasechnic, I. A. Korzh and E. N. Mozhzhukhin, Scattering Cross Sections of Neutrons up to 3.0 MeV by Chromium, Iron and Nickel Isotopes, Int. Conf. on Nuclear Cross Sections for Tech., N.B.S. Special Publication 594, Knoxville, Tennessee (1979).
4. B. Holmqvist and T. Wiedling, "Neutron Elastic Scattering Cross Sections: Experimental Data and Optical Model Cross Section Calculation. A Compilation of Neutron Data from the Studsvik Neutron Physics Laboratory." Aktiebolaget Atomenergi Report AE-366 (1969).
B. Holmqvist and T. Wiedling, "Neutron Elastic Scattering Studies of Chromium, Iron and Nickel in the Energy Region 1.77 to 2.76 MeV," Aktiebolaget Atomenergi Report AE-385 (1970).
5. O. A. Salnikov, Angular Distribution of 2.35 MeV Neutrons Scattered Elastically by Chromium, Iron and Lead, Atomnaya Energiya, 3, 106 (1957).
6. R. L. Becker, W. G. Guindon and G. J. Smith, Elastic Scattering of 3.2 MeV Neutrons from Many Elements, Nucl. Phys., 89, 154 (1966).
7. E. Almén-Ramström, "A Systematic Study of Neutron Inelastic Scattering in the Energy Range 2.0 to 4.5 MeV", AE-503, Studsvik, Nyköping, Sweden (1975).
8. D. M. Van Patter, N. Nath, S. M. Shafroth, S. S. Malik, and M. A. Rothman, Phys. Rev., 128, 1246 (1962).
9. D. L. Broder, V. E. Kolesov, A. I. Lashuk, I. P. Sadokhin, and A. G. Dovbenko, Sov. J. At. Energy, 16, 113 (1964).
10. R. E. Coles, "(n,n' γ) Reactions in Natural Chromium", AWRE O-41/71, U.K. Atomic Energy Authority, Aldermaston (1971).
11. P. T. Karatzes, et al., Nucl. Sci. & Eng., 67, 34 (1978).
12. G. Tessler and S. S. Glickstein, Proc. Conf. Nuclear Cross Sections and Technology, NBS Special Publication 425, p. 934, National Bureau of Standards (1975).

13. F. Voss, S. Cierjacks, D. Erbe, and G. Smalz, Proc. Conf. Nuclear Cross Sections and Technology, NBS Special Publication 425, p. 916, National Bureau of Standards (1975).
 14. P. T. Guenther, W. P. Poenitz and A. B. Smith, "Interpretation and Normalization of Experimental Data for Total, Scattering and Reaction Cross Sections," Workshop on Evaluation Methods and Procedures DOE - Brookhaven National Laboratory, Upton, New York (1980).
 15. A. Prince and T. W. Burrows, "Evaluation of Natural Chromium Neutron Cross Sections for ENDF/B-V," BNL-NCS-51152 (ENDF 286), National Neutron Cross Section Center, Brookhaven National Laboratory, Upton, New York (1979).
 16. Metron Inc., Alamucky, New Jersey
 17. S. A. Cox and P. R. Hanley, IEEE Trans. Nucl. Sci., NS-18, No. 3, 108 (1971).
 18. A. Smith and J. Whalen, Comments on Energy-Averaged Neutron Total Cross Sections, Argonne National Laboratory Report, ANL/NDM-33 (1977).
 19. D. Miller, Fast Neutron Physics, Vol. II, Eds. J. Marion and J. Fowler, Interscience Pub., New York (1963).
 20. R. B. Schwartz, R. A. Schrack and H. T. Heaton, II, "MeV Total Neutron Cross Sections," U.S. Natl. Bur. Stds. Pub. NBS-138 (1974).
 21. S. Cierjacks, P. Forti, D. Kopsch, L. Kropp, J. Nebe and H. Unfeld, "High Resolution Total Neutron Cross Sections between 0.5-30 MeV," Karlsruhe Report, KFK-1000 (1968).
 22. G. D. James, Proc. Sym. on Neut. Stds., U.S. Natl. Bur. of Stds., Pub. NBS Special Publications 493 (1977).
 23. A. B. Smith, P. Guenther, R. Larson, C. Nelson, P. Walker and J. F. Whalen, Nucl. Instr. and Methods, 50, 277 (1967)
- See also
- P. Guenther, A. Smith and J. Whalen, Phys. Rev., C12, 1797 (1975).
 24. A. Smith, P. Guenther and R. Sjoblom, Nucl. Instr. and Methods, 140, 397 (1977).
 25. J. Hopkins and G. Breit, Nucl. Data, A9, 137 (1971).
 26. P. T. Guenther, Univ. of Illinois Thesis, Elastic and Inelastic Neutron Scattering from the Even Isotopes of Tungsten (1977).
 27. Evaluated Nuclear Data File - B(ENDF/B) Version-V, National Nuclear Data Center, Brookhaven National Laboratory, Upton, New York (1979).

28. J. A. Harvey et al., private communication, data available from the National Nuclear Data Center, Brookhaven National Laboratory, Upton, New York (1979).
29. W. Hauser and H. Feshbach, Phys. Rev., 87, 366 (1952).
30. Nuclear Level Schemes A=45 through A=257 from Nuclear Data Sheets, Edited by Nuclear Data Group, Oak Ridge National Laboratory, Academic Press (1973).
31. P. Hodgson, The Optical Model of Elastic Scattering, Oxford Press, London (1963).
32. ABAREX, Digital Computer Program, P. A. Moldauer, private communication (1979).
33. JUPREX, Digital Computer Program, P. A. Moldauer, private communication. (1979).
34. A. B. Smith, P. T. Guenther and J. F. Whalen, Fast-Neutron Scattering Cross Sections of Cr, Fe and Ni, Int. Conf. on Nuclear Cross Sections for Tech., NBS Special Publication 594, Knoxville, Tennessee, (1979).
35. A. Smith and P. Guenther, "Scattering of MeV Neutrons from Elemental Iron," Argonne National Laboratory Report, ANL/NDM-47 (1979).

FIGURE CAPTIONS

Fig. 1. Extrapolation of Effective Neutron Total Cross Sections.

- a) The lower portion of the figure shows the extrapolated energy-averaged cross sections of elemental Cr as stars, those of the Cr ENDF/B-V as squares (see text for details). The upper portion of the figure details the linear fit to the effective cross sections at each energy point as deviation from the extrapolated (i.e., "zero thickness") values in percent vs. sample thickness (nuclei per barn).
- b) Simulated extrapolation derived from the Cr ENDF/B-V total cross sections using the energy resolution of the present work.
- c) As in b) but using the high-resolution Fe data of [28].
- d) As in c) but with a 10 keV resolution.

Fig. 2. Neutron Total- and Elastic-Scattering Cross Sections of Elemental Chromium. The present results are indicated by 0 and \square , those of [3] by x, those of [4] by +. The light curves are the corresponding appropriately averaged ENDF/B-V values. The heavy curves are the results of model calculations of this work.

Fig. 3. Neutron Elastic-Scattering Angular Distributions for Elemental Chromium. The curves are Legendre polynomial least-squares fits to the combined experimental data. (Units: Barns per steradian in laboratory degrees.)

Fig. 4. Neutron Elastic-Scattering Angular Distributions for Elemental Chromium. The results of this work (0) are compared with those of [3] (x) and [4] (+) at selected incident-neutron energies. The parenthetical energy values pertain to [4]. The curves are least-squares Legendre polynomial fits to the ± 200 keV average of the present data. (Units: Barns per steradian in laboratory degrees.)

Fig. 5. Neutron Inelastic-Scattering from Elemental Chromium. The cross sections of this work (0) are compared with those of [3] (x), those of [7] (+), and summed entries from ENDF/B-V as described in the text (light curves). The heavy curves are the results of model calculations of this work.

Fig. 6. Neutron Elastic-Scattering Angular Distributions for Elemental Chromium. Experimental data of this work have been averaged over ± 200 keV intervals and are indicated by 0. The curves are the results of model calculations of this work. (Units: Barns per steradian in laboratory degrees.)

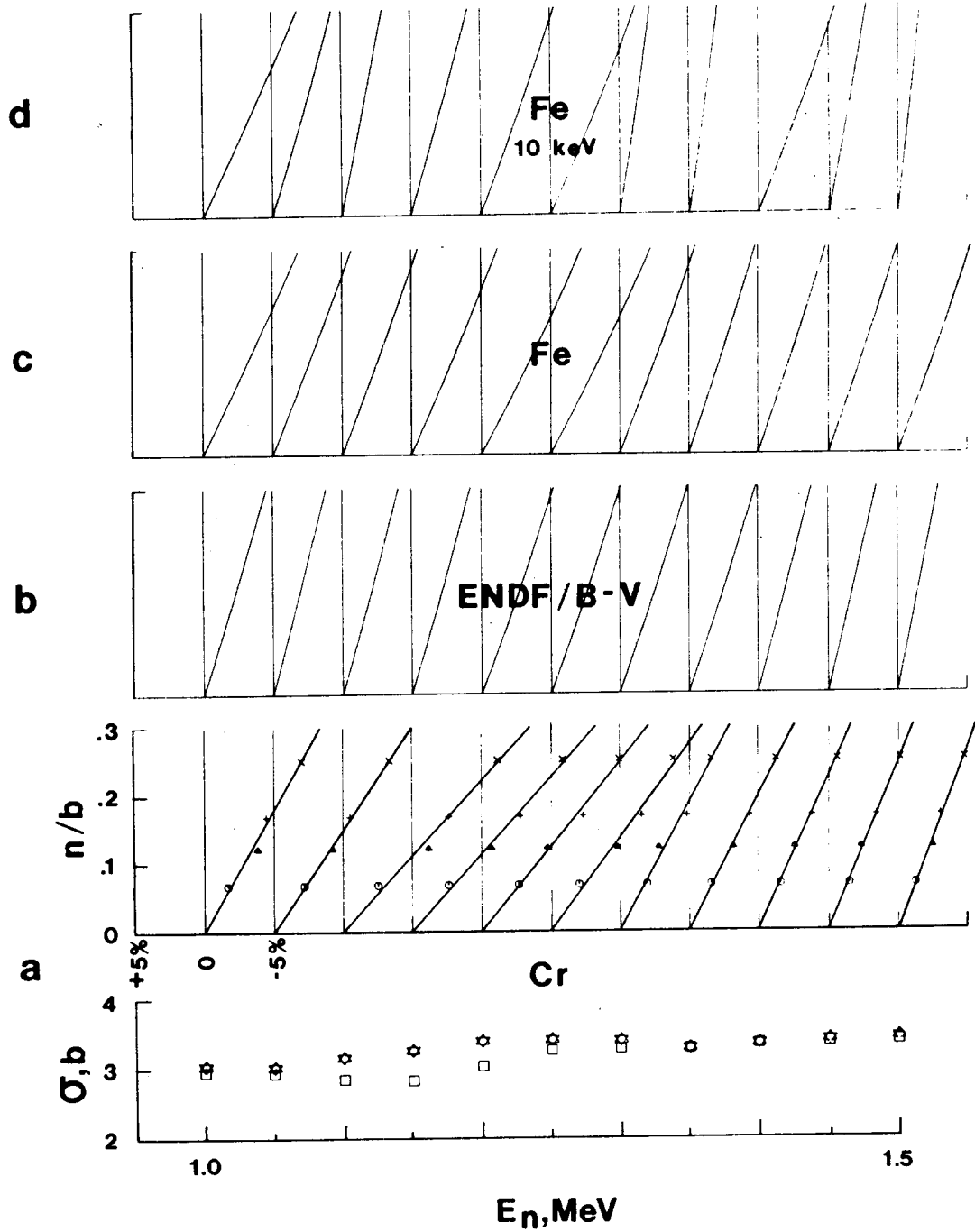


Figure 1.

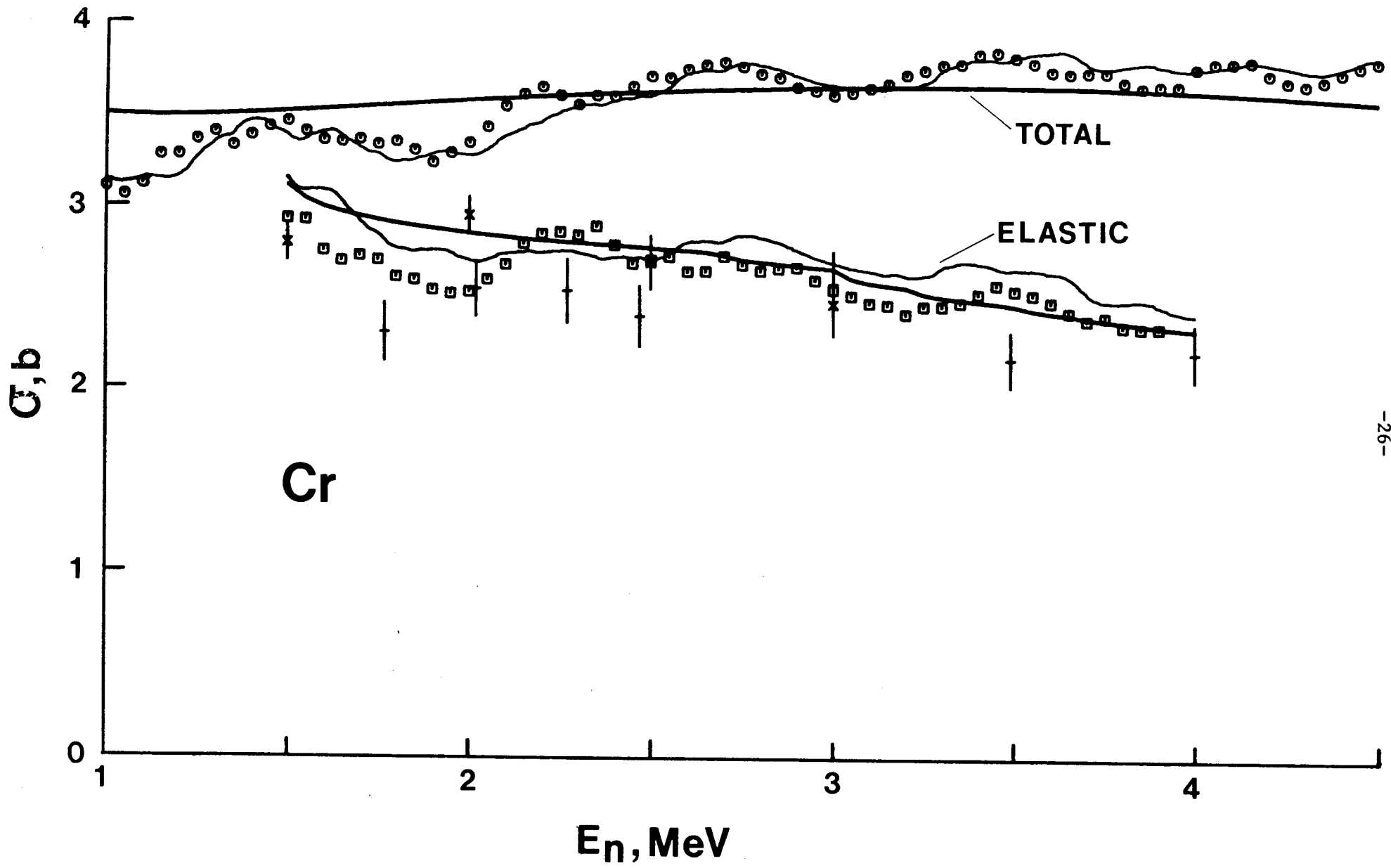


Figure 2.

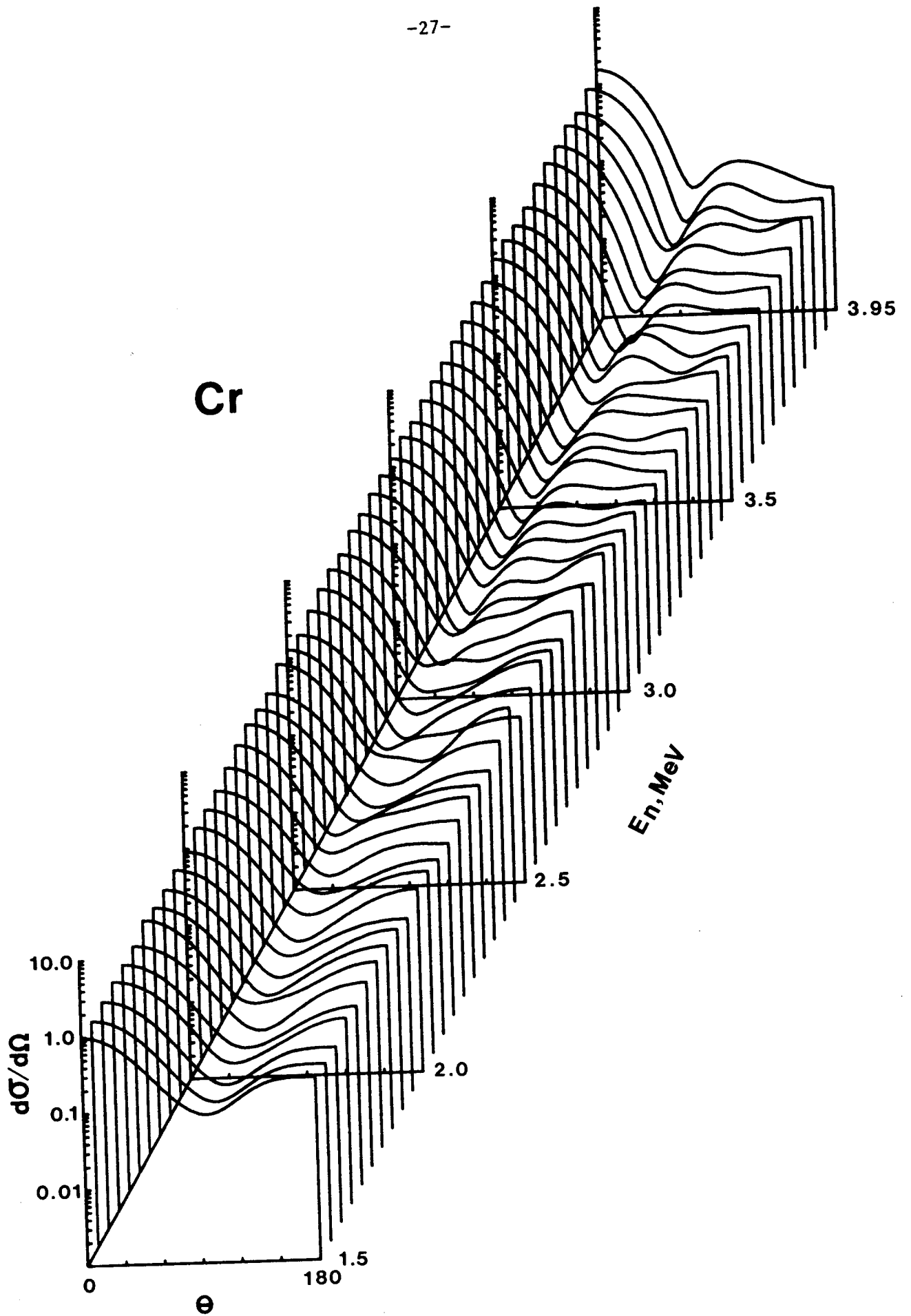


Figure 3.

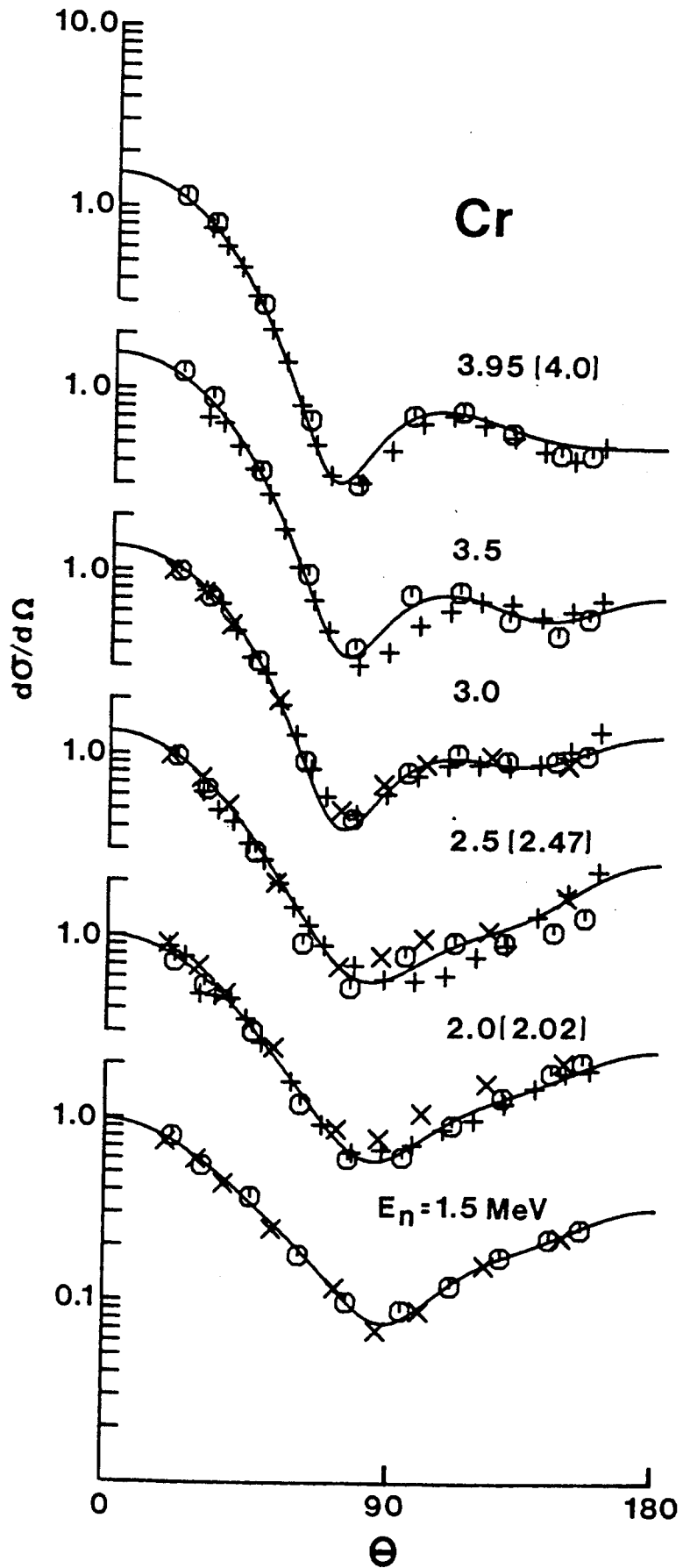


Figure 4.

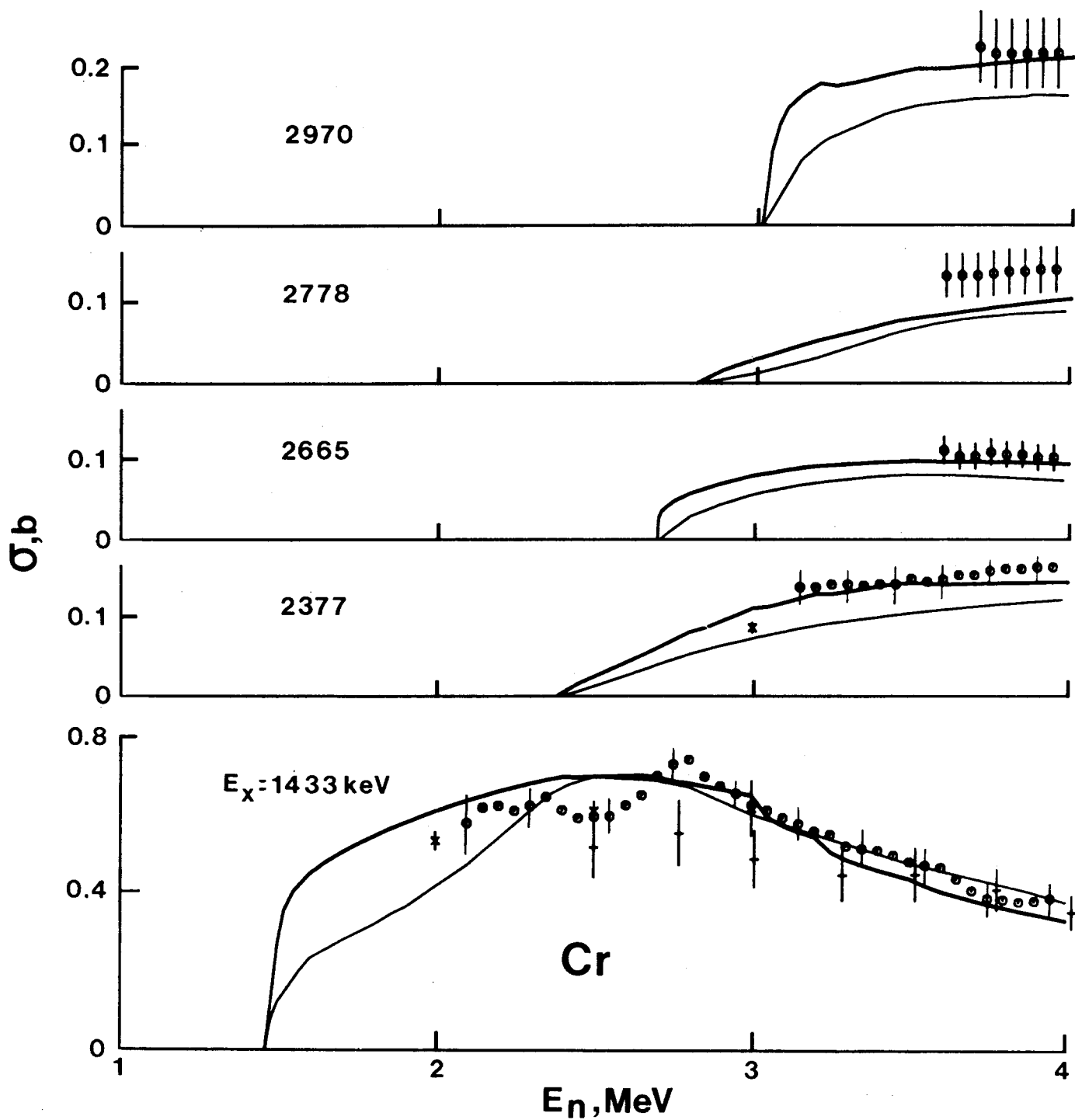


Figure 5.

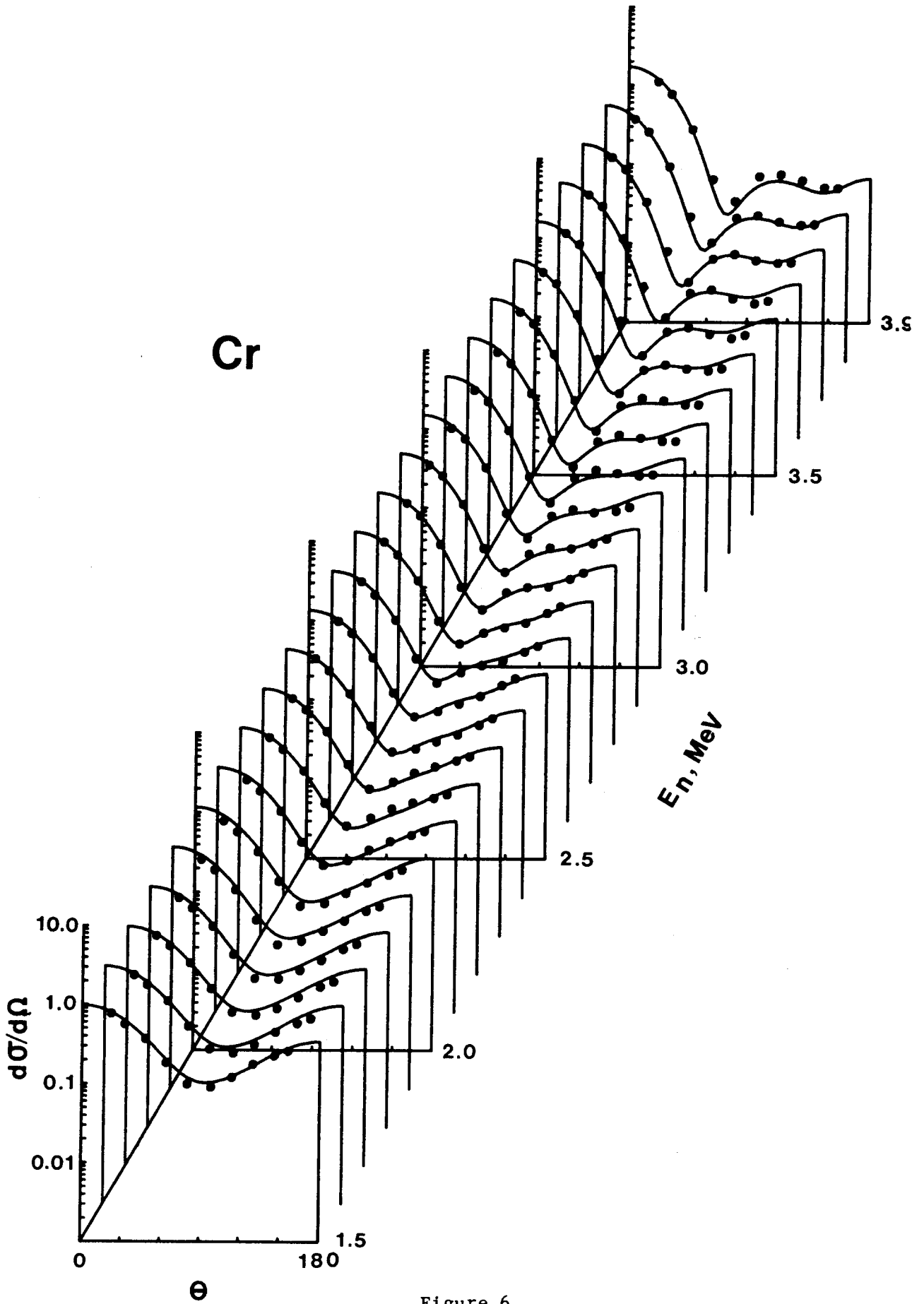


Figure 6.